ROBUST PSS DESIGN FOR MULTI MACHINE POWER SYSTEM USING H_∞ LOOP SHAPING TECHNIQUE

Jayapal REDDY
R.V. College of Engineering, Bengaluru, Karnataka, India, Email:rv_rj@rediff.com
Mendiratta JUGAL KISHORE
C.M.R. Institute of Technology, Bengaluru, ISE Dept., Karnataka, India, Email: mendiratta.jk@gmail.com

Abstract — *This paper describes a novel method of designing an H_∞ loop shaping based Robust Power System Stabilizer (RPSS) for multi-machine power system. Based on the latest development of non-linear H_∞ robust control theory, a control design is applied to stabilize the linearized uncertain system using Glover-McFarlane loop shaping technique. In this paper, RPSS design is presented for IEEE 10 machine 39 bus system, using Glover-McFarlane H_∞ loop shaping technique. Guidance for setting the feedback configuration for loop shaping and synthesis are also presented. After obtaining the controller, non-linear simulations are performed and comparisons of the performances are made with the Conventional PSS (CPSS) and the resulting RPSS for a 3-phase fault. The justification of robustness is also provided by comparing RPSS with CPSS by considering 3 different operating points.*

Key words — *H_∞ loop shaping, Power system stabilizer, Multi machine power system, Robust controller, State space.*

1. Introduction

The main objective of installing Power System Stabilizer (PSS) is to achieve desired stability and security at a reasonable cost by adding damping to electromechanical oscillations and to enhance power transfer limits. Conventional stabilizers are not designed in a way to guarantee the desired level of robustness. Such designs are specific for a given operating point; they do not guarantee robustness for a wide range of operating conditions. The dynamics of a multimachine power system are both nonlinear and interconnected. The equilibrium of such a system is typically unknown and uncertain and the controllers within are also subjected to physical limitations. In recent years there has been an increasing interest on applying advanced control designs in power systems like adaptive control, H_∞ control, μ synthesis, nonlinear control, feedback linearization, fuzzy logic control and neural control [1]. The goal of these studies is to achieve stability and performance robustness.

To include the model uncertainties at the controller design stage, modern robust control methodologies have been used in recent years to design PSS [2].The resulting PSS ensures the stability for a set of perturbed operating points with respect to the nominal system and has good oscillation damping ability. The proposed controller is free from common deficiencies of power system nonlinear controllers as network dependence and equilibrium dependence.

The H_∞ optimal controller design is relatively simpler in terms of the computational burden. This paper uses the Glover-McFarlane H_∞ loop shaping design procedure with the normalized coprime factor robust stabilization method [3] to design the RPSS. This design procedure is applied to design RPSS for IEEE 10 machine 39 bus system and provide some basic guidelines for loop shaping, weighting selection and controller design paradigm formulation.

A number of researchers had worked on power system stabilizers. Attempts are made for RPSS design using H∞ loop shaping method, proposed by McFarlane and Glover, with the normalized coprime factor robust stabilization method for SMIB systems. This method is attempted for multimachine system based on sequential tuning [1]. No attempts are made to implement this method for multimachine system based on simultaneous tuning. The proposed method is effectively applied to design RPSS based on decentralized scheme with simultaneous tuning.

The paper is organized in the following sequence. In Section 2, the power system model description and the problem statement are provided. In Section 3, the controller design paradigm is given with a greater detail, relating to the concepts of the H_∞ controller. The detailed simulation results are presented in Section 4 along with the justification of robustness by comparing RPSS with CPSS and in Section 5, the conclusions are provided. This is followed by the references & the appendix.

2. Development of the power system model

In this paper, the synchronous machine is modeled using Model 1.1 [4] in which case one field winding on *d*-axis and one equivalent damper on *q*-axis are considered. The relevant equations [4] of model 1.1 are provided in Appendix A. The multimachine power system is modeled using Simulink Toolbox of Matlab and the same is shown in Fig.18, in the Appendix B. A linear state space model is obtained for the same using the function LINMOD available in Matlab. To study the control of power system oscillations, IEEE 10-machine, 39 bus system, taken from [4] is used. The single line diagram of the system is as shown in Fig.20, in the Appendix C.

Table 1 Eigen values of The System

Swing mode	Without PSS
M1	−0.4518 ± 8.7079i
M2	−0.583 ± 8.5765i
M3	−0.54362 ± 7.6758i
M4	−0.17556 ± 7.2476i
M5	−0.25643 ± 6.7783i
M6	−0.0092673 ± 6.1157i
M7	0.31593 ± 5.6748i
M8	0.0076043 ± 3.7055i

The Table 2 gives the participation factors (magnitude) of the system corresponding to modes M1 to M8 (*- indicates very small values of participation factors). The participation factors are the product of left eigenvector and right eigenvector of the system for a given mode [6].The model matrix, M, of the system is obtained using [M, E] =eig (A). The absolute value of the product of the inverse of M and M corresponding to the given mode gives participation factors of that mode. The speed of that machine with highest participation in a particular mode is the best signal to damp the oscillations due to that mode. In Table 2, Smi correspond to slip of the i^{th} machine. The prominent participation factors are highlighted in the table. It can be observed from Table 2, that, generators 5, 7, 8, 1, 4, 3, 9 and 2 control the swing modes M1, M2, M3, M4, M5, M6, M7and M8 respectively and the participation factors of generators 2, 3, and 4 are insignificant. Hence generators 1, 5, 7, 8 and 9 are the best locations to place PSSs to damp modes M1 to M8.

Table 2 Participation factors

Mode	Sm1	Sm2	Sm3	Sm4	Sm5	Sm6	Sm7	Sm8	Sm9	Sm10
M1	*	*	*	0.1063	**0.2835**	0.0210	0.1096	*	*	*
M2	*	*	*	0.0457	0.0721	0.1739	**0.2312**	*	*	*
M3	*	*	*	*	*	0.0117	*	**0.4657**	0.0212	0.0612
M4	**0.2806**	*	0.2205	*	*	*	*	*	*	*
M5	*	*	*	**0.2107**	0.0426	0.1894	0.0751	*	*	*
M6	0.1596	*	**0.1972**	0.0615	0.0260	0.0309	0.0164	*	*	*
M7	0.0123	*	0.0179	0.0260	0.0150	0.0211	0.0128	*	**0.3679**	*
M8	0.0158	**0.1933**	0.0251	0.0479	0.0432	0.0576	0.0414	0.0116	0.0528	0.0113

If the PSS design is based on the one machine infinite bus model, after the installations of PSSs on most machines of a large power system, low frequency oscillations may still occur due to lack of coordination of these stabilizers [5]. Hence, coordinated application of PSSs is required. To achieve the coordination, the state matrix of the entire system is used to design PSS using Glover-McFarlane H_∞ loop shaping design procedure. For the system considered this procedure yields ten stabilizers one at each machine. Using the method explained in section 3, one of the ten stabilizers is selected. Using participation factor technique [6], [7] stabilizers are placed only at the machines where PSS is most essential.

For the example considered, the eigenvalues associated with the eight modes at the given operating point without PSS are given in Table 1. The eigenvalues are obtained using the function eig(A) available in Matlab, where A is the state matrix of the system. The swing modes are the eigenvalues close to jω-axis in the s-plane. From Table 1, it can be observed that the system has two positive eigenvalues corresponding to swing modes M7 and M8. Hence the system is unstable under normal operating conditions, necessitating the requirement of PSS.

3. Robust Controller Design

To start with, a brief review of the design procedure relating to the design of the robust H_∞ controller based on Glover-McFarlane H_∞ loop shaping technique is presented. This is followed by the design of the robust power system stabilizer (RPSS) for the multi-machine power system using this technique.

3.1 Review of the procedure for robust controller design

Among many robust control techniques, H_∞ control theory is one of an excellent robust technique for designing RPSS. Based on this theory, three techniques of RPSS design are possible using (i) H_∞ optimal controller (ii) H_2/ H_∞ mixed sensitivity controller and (iii) H_∞ loop shaping controller.

RPSS design using H_∞ optimal controller theory is tedious and so, in practice a suboptimal rather than optimal solution is used. However, this H_∞ design procedure produces undesirable controllers whose zeros cancel all the stable plant poles, which is unacceptable when the plant contains lightly damped modes [8]. The design of H_∞ PSS via mixed sensitivity approach reveals the high performance and robustness but the selection of weighting functions poses a problem due to the trade off relationship between sensitivity function and complementary sensitivity function [9].

The loop shaping is conceptually simple yet powerful design method in the frequency domain. The constraints of the loop phase near crossover frequency (stability requirements) complicate the loop shaping procedure considerably either for systems with RHP poles and zeros or for the multi input and multi out (MIMO) case. In the present work, PSS is designed by modifying the third technique based on the Glover–McFarlane H_∞ loop shaping design procedure [3]. This method combines the advantages of loop shaping and H_∞ control via normalized coprime factorization (NCF) approach. This design procedure follows the classical loop shaping principles in the choice of the control objectives, while the stability requirement is embedded into a special robust stability framework called NCF robust stability problem. In contrast to the classical loop shaping approach, the loop shaping is done without explicit regard to the nominal plant phase information. The present design is both simple and systematic in terms of design and weighting function selection.

The Glover-McFarlane H_∞ loop shaping design procedure [3], [1] consists of the following 3steps:

a. ***Loop shaping:*** If G is the nominal plant and K is the controller, then using a pre-compensator W_1 and/or a post compensator W_2, the singular values of the nominal plant are shaped to give a desired open-loop shape. This step takes advantage of the conventional loop shaping technique, but no phase requirements need to be considered. That is, the closed-loop stability requirements are disregarded since the H_∞ synthesis step taken thereafter will robustly stabilize the shaped plant. This ensures acceptable level of performance as well as stability in the face of perturbations. W_1 is selected to keep the sensitivity $S = (I + GK)^{-1}$ (1)
low at low frequencies such that

$$\left\| W_1^{-1} S \right\|_\infty \le 1, \quad (2)$$

while W_2 is selected to keep the complementary sensitivity

$$T = GK\,(I + GK)^{-1} \quad (3)$$

low at high frequencies such that

$$\left\| W_2^{-1} T \right\|_\infty \le 1. \quad (4)$$

This ensures acceptable level of performance as well as stability in the face of perturbations. The nominal plant G and shaping functions W_1, W_2 are combined to form shaped plant, $G_s = W_2\, G\, W_1$. It is assumed that W_1 and W_2 are such that G_s contains no hidden modes.

b. ***Robust Stabilization:*** It has been shown that the largest achievable stability margin ε_{max} can be obtained by a non-iterative method [3], [10]. Here, ε_{max} is the stability margin for the normalized co-prime factor robust stability problem [10]. It provides a robust stability guarantee for the closed loop system. Suppose $\tilde{M}_s, \tilde{N}_s$, are normalized left co-prime factors of G_s such that $G_s = \tilde{M}_s^{-1}\tilde{N}_s$ (6)

then, $$e_{max} = \left(1 - \left\| \tilde{M}_s \tilde{N}_s \right\|_H^2\right)^{1/2} \quad (7)$$

where, $\|\cdot\|_H$ denotes the Hankel norm. The controller is now defined by selecting $\varepsilon <= \varepsilon_{max}$ and then synthesizing a stabilizing controller K_∞, which satisfies $$\left\| \begin{bmatrix} I \\ K_\infty \end{bmatrix} (I - G_s K_\infty)^{-1} \tilde{M}_s^{-1} \right\|_\infty \le \varepsilon^{-1} \quad (8)$$

as shown in the Fig. 1a.

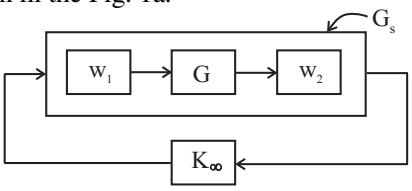

Fig.1a: Block diagram of the shaped plant & K_∞ controller.

$\|\cdot\|_\infty$ denotes the H_∞ norm, which is the supermum of the largest singular value over all frequencies. If $\varepsilon_{max} << 1$, return to step (a) and adjust W_1 and W_2.

c. ***The final feedback controller K*** is then constructed by combining the H_∞ controller K_∞ with the shaping functions W_1 and W_2 such that $K = W_1 K_\infty W_2$, which is shown in the Fig. 1b.

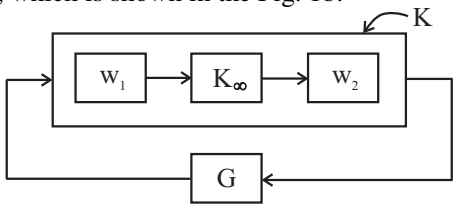

Fig.1 b Final controller $K = W_1 K_\infty W_2$

3.2 Design of R PSS for the multi-machine power system

The highlighted procedure is then applied to the multi-machine power system considered.

A. ***Loop Shaping:*** The state matrix representation of the system is obtained. The Eigen values of this system correspond to the inter-area mode. The damping ratio of the system is computed. The system has poor damping at frequency 3.71 and 5.68 rad/sec. The objective of loop shaping is to increase the open-loop gain around this frequency [1].

Selection of W_1: Pole and zero pairs are added to achieve gain increase in the desired frequency range while keeping the gain change as small as possible around other frequency values [1]. A washout filter block in W_1 with time constant 15 sec. is used to ensure the controller only works in the transient state [6]. The selection of the pole at 1/0.2695 and the zero at 1/0.33 increased the gain around the frequencies of interest so that the plant input disturbance can be attenuated effectively. The resulting transfer function for the shaping function

$$W_1 = \frac{100\times 15s\times(1+0.33s)}{(1+15s)(1+0.2695s)(1+0.1761)}.$$

Selection of W_2: With $W_2 = 1$, the open loop gain $G_s = W_2 G W_1$ was very less and more over, the slope of the shaped plant was low at low frequencies. To increase the gain of the system at low frequency, three repeated zeros are added at frequency of 10 rad/sec. To make W_2 proper and to achieve proper slope of G_s at cross over frequency, three poles are added at insignificant frequency of 300 rad/sec. The reduced DC gain of W_2 is compensated by using a constant of value of 10000 [1]. The resulting transfer function for the shaping function

$$W_2 = \frac{10000\times(s+10)^3}{(s+300)^3}.$$

The resulting singular value plot of the nominal system G, W_1, W_2 and G_s are as shown in Fig. 2.

B. ***H_∞ synthesis:*** Next, we synthesized a K_∞ controller to achieve robust stability for the nominal plant. From the equation $e_{\max} = \left(1 - \left\|\left[\tilde{M}_s \tilde{N}_s\right]\right\|_H^2\right)^{1/2}$, the maximum stability margin is $\varepsilon_{\max} = 0.2473$. This margin evaluates the feasibility of our loop shaping design.

According to McFarlane and Glover [3], [10], given the normalized left coprime factorization of the nominal plant as $G_{s_0} = \tilde{M}_s^{-1}\tilde{N}_s$, the controller K_∞ can stabilize all $G_s = (\tilde{M} + \Delta_M)^{-1}(\tilde{N} + \Delta_N)$ satisfying $\left\|\Delta_M, \Delta_N\right\|_\infty < 0.2473$. Furthermore, this controller stabilizes a gap ball of uncertainty with a given radius if and only if it stabilizes a normalized coprime factor perturbation ball of the same radius. Thus, in terms of the gap metric, all G_s with $\delta_g(G_s, G_{s_0}) < 0.2473$ can be stabilized by this controller.

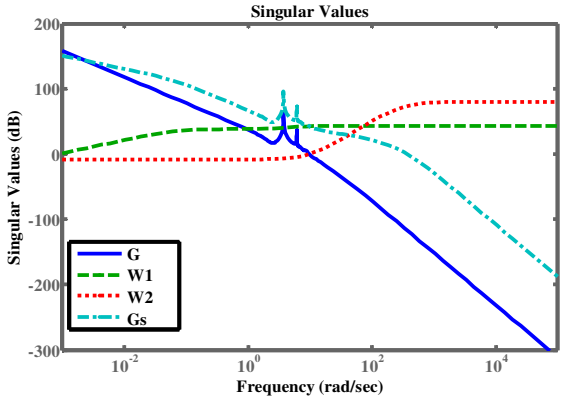

Fig.2 The singular value plot of G, W_1, W_2 and G_s

C. **The final controller K:** The final controller is the combination of W_1 and W_2 with K_∞, that is $K = W_1 K_\infty W_2$. This gives 10 controllers from 10 inputs to the output such as K (1, 1), K (1, 2) ….. K (1, 10). To find the best of the 10 controllers, Bode magnitude plot of each controller is compared with the Bode magnitude plot of general controller K. The controller whose Bode magnitude plot closely matches with the Bode magnitude plot of general controller is selected as the best controller. For the example considered, K (1, 9) matches with the general controller K as shown in Fig. 3.

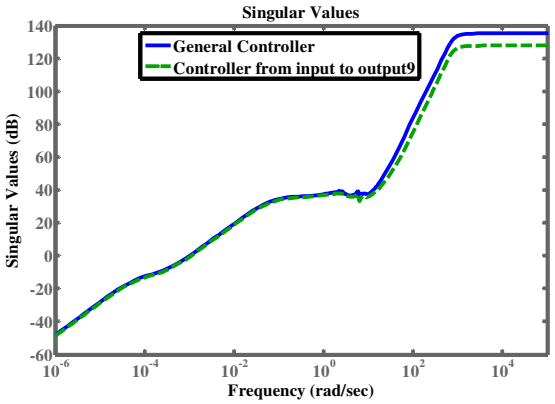

Fig. 3 The singular value plot K and $K(1, 9)$

D. Controller order reduction

The designed controller is of a high order. It is required to reduce it to a lower order for practical implementation purposes [11]. The controller is reduced to a 7^{th} order using the Hankel norm reduction method. The transfer function of the reduced order controller is given as

$$K=\frac{\left\{\begin{array}{l}2.46*10^{6}s^{7}+2.542*10^{9}s^{6}+9.494*10^{11}s^{5}+1.452*10^{14}s^{4}+\\7.403*10^{15}s^{3}+1.312*10^{17}s^{2}+9.426*10^{17}s+1.146*10^{16}\end{array}\right\}}{\left\{\begin{array}{l}s^{7}+2541s^{6}+3.205*10^{6}s^{5}+2.349*10^{9}s^{4}+9.754*10^{11}s^{3}\\+2.047*10^{14}s^{2}+1.678*10^{16}s+9.807*10^{14}\end{array}\right\}}$$

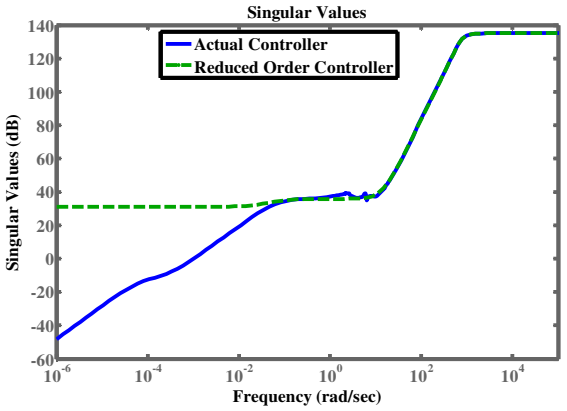

Fig.4 Bode plot of the actual and reduced order controller

The bode plots of the full-order controller and the reduced-order controller are shown in Fig.4. The reduced order controller exactly matches with the original controller at the frequencies of interest. We note that the gain of the controller does not roll off rapidly at high frequencies. After adding the designed controller, the damping of the nominal closed-loop system has increased. This is implemented at generators 1, 5, 7, 8 and 9 as shown in Fig.19, shown in Appendix B.

4. Simulation results

Nonlinear simulations are performed using the developed Simulink model and comparisons are made w.r.t. the following 2 cases, viz,

(i) With & without RPSS (*without any fault*).
(ii) Comparison of RPSS with CPSS (*With fault*).

4.1 With & without RPSS (without any fault)

Prior to application of fault, simulation is carried out with and without RPSS and without any fault i.e., under steady state condition. The simulation results of rotor angles and relative slip of all generators with respect to Centre of Inertia (COI) are plotted individually but results are shown only at few generators. The rotor angle and relative slip plots at other generators are similar hence are not shown here.

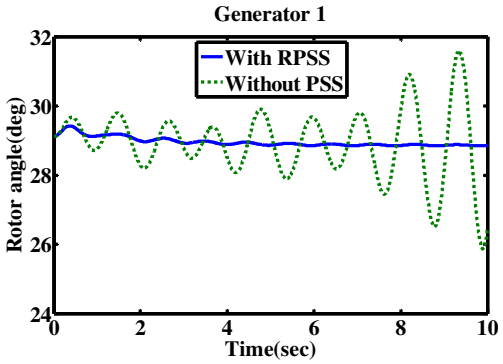

Fig.5 Rotor angle at generator 1 with and without RPSS under steady state

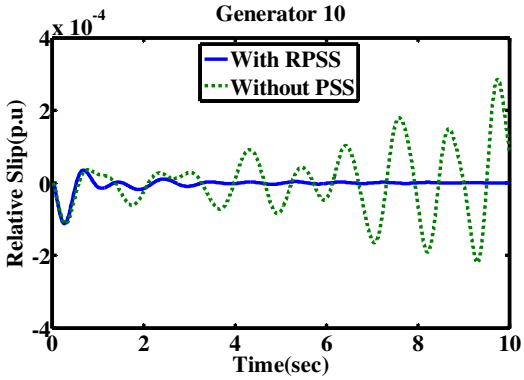

Fig.6 Relative slip at generator10 with and without RPSS under steady state

Fig.5 shows the variation of rotor angle under steady state condition at the generator 1 whereas Fig.6 shows the variation of relative slip with respect to COI under steady state condition at generator10. From these plots it can be observed that the system is unstable under steady state condition which is justifiable as the system has two positive eigenvalues corresponding to swing modes M7 and M8, which

can be seen from the Table 1. The system becomes stable with the addition of robust controller. The transients vanish within 2 to 3sec with the presence of RPSS.

As the system is unstable without PSS under steady state condition, it will be highly unstable during fault and hence its performance is not compared without controller during fault.

4.2 Comparison of RPSS with CPSS (With fault):

Next, a three Phase to ground fault is created at a line connected between the buses 26 and 29 near bus no. 29 as shown in the Fig.20. The fault is initiated after 1 second and automatically cleared at the end of 5 cycles. The non-linear simulations are performed at different generators. The simulation results of RPSS are compared with CPSS and the response curves of rotor angle, slip and torque are observed at all the generators but only few results are shown here due to want of space. The details of CPSS are provided in the Appendix D.

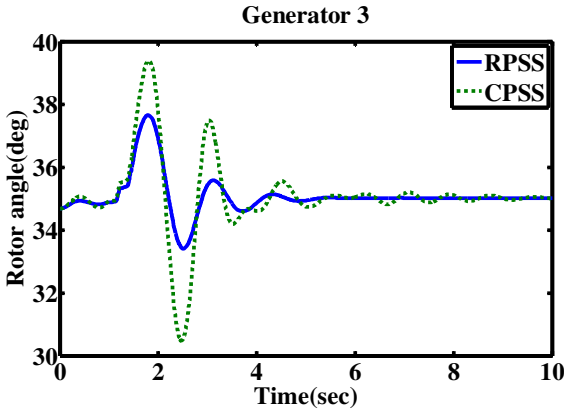

Fig.7 Rotor angle of generator 3 with RPSS and CPSS with a three phase fault

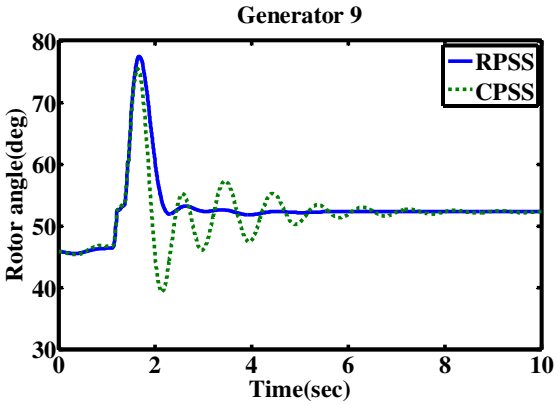

Fig.8 Rotor angle of generator 9 with RPSS and CPSS with a three phase fault

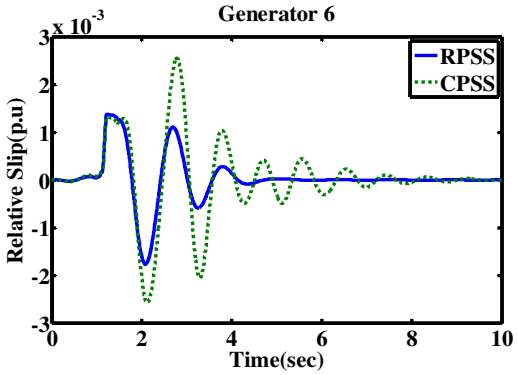

Fig.9 Relative slip at generator 6 with RPSS and CPSS with a three phase fault

The variations of rotor angles vs. time at generators, say, 3 & 9 are plotted randomly and are shown in the Fig.7 & Fig.8 respectively. The variation of relative slip vs. time at generator 6 is plotted and the same is shown in the Fig.9. Similarly the simulation result of electric torque at generator 9 is shown in Fig.10. As shown in these plots, the proposed RPSS is able to damp out the oscillations consistently within 3 to 4 seconds after clearing the fault is cleared, while CPSS takes longer time to bring the system to steady state condition. This indicates the effectiveness of RPSS in providing the required damping to the system.

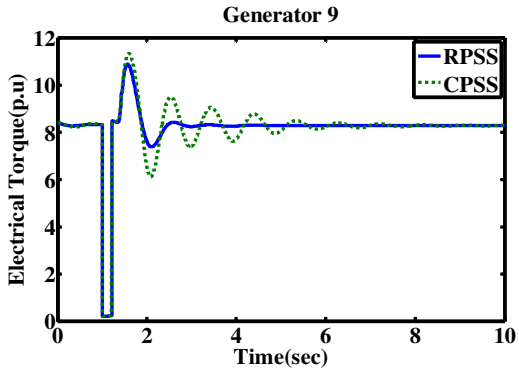

Fig.10 Electric torque at Generator 9 with RPSS and CPSS with a three phase fault

4.3 Justification of Robustness

For justification of robustness the following operating loads as three cases are considered.

Case 1: 2.0 times the original loads.

Case 2: 2.5 times the original loads and

Case 3: 3.0 times the original loads.

The Fig.11to Fig.16 indicate the responses which are observed randomly at few generators when the system is subjected to the above faults considered as case 1, case 2 & case 3.

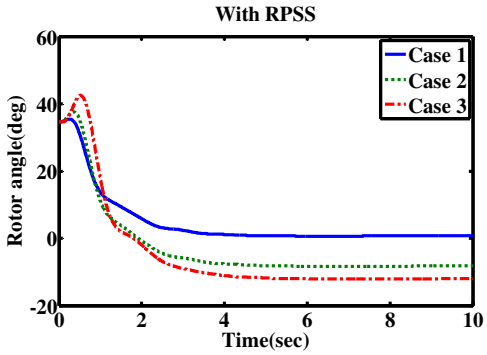

Fig.11 Rotor angle of generator3 with RPSS for three different operating points

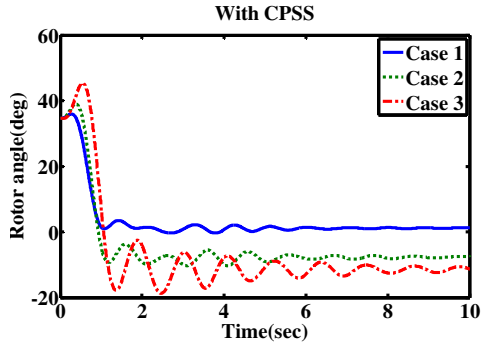

Fig.12 Rotor angle of generator3 with CPSS for three different operating points

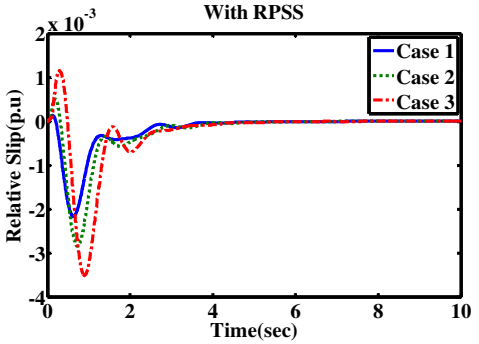

Fig.13 Relative Slip of generator 1 with RPSS for three different operating points

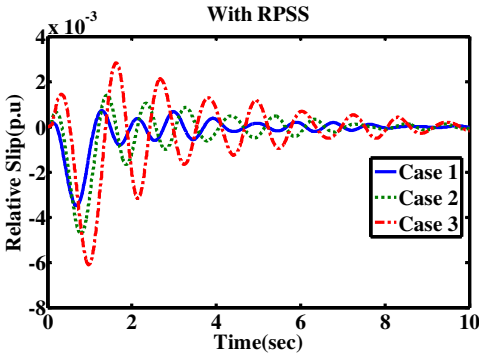

Fig.14 Relative Slip of generator 1 with CPSS for three different operating points

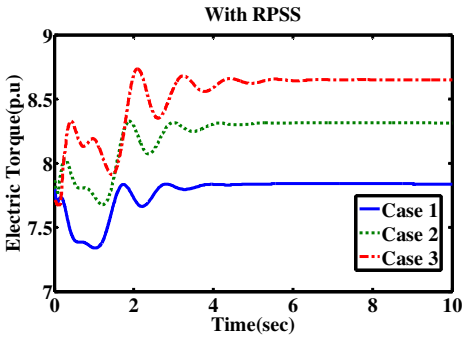

Fig.15 Electric torque of generator5 with RPSS for three different operating points

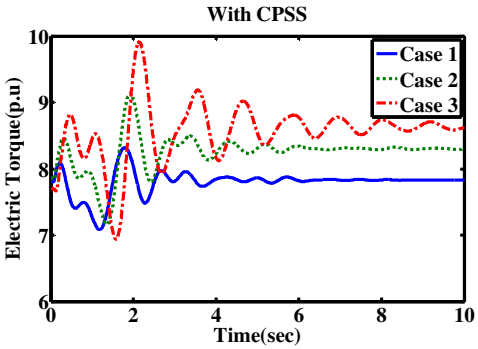

Fig.16 Electric torque of generator5 with CPSS for three different operating points

Figs11, 13 and 15 show the variation of rotor angle at generator3, relative slip at generator1 and electric torque at generator5 respectively, for the three different operating points considered with RPSS, while Figs12, 14 and 16 show the variation of rotor angle at generator3, relative slip at generator1 and electric torque at generator5 respectively, for exactly the same conditions with CPSS. From these plots, it can be clearly seen that in case of the system with RPSS, the settling time is consistently small and is almost independent of the operating point and the system is subjected to less oscillations, justifying robustness. In the case of the system with CPSS, the settling time varies inconsistently with the change in operating point and the system is subjected to large transients indicating the system fails to achieve robustness.

5. Conclusions

A systematic approach to design PSS using Glover-McFarlane H_∞ loop shaping technique is presented for an IEEE 10 machine, 39 bus multi-machine power system. A generalized Matlab program was developed for the multi-machine power system for calculation of initial conditions and a generalized Simulink model was developed for the

integrated multi-machine power system.

Non-linear simulations were performed for a period of 10 sec with & without RPSS model under steady state conditions. Various performance characteristics such as the rotor angle, slip and electric torque were observed. Comparisons of the performance characteristics were made with CPSS & with RPSS with a 3-phase to ground fault, to show that the transients die out very quickly with RPSS, while they exist for a longer duration with the CPSS. Robustness justification with RPSS was also dealt by showing that the settling time is independent of the operating point, while the settling time in case of CPSS varies depending upon the operating point, failing to achieve robustness.

Simulations demonstrate the good damping performance of the designed RPSS, while the design procedure used is much simpler. Collectively, these results show that the RPSS provides better damping and robustness under fault conditions. The above procedure can be applied to large multi-machine / intra-area power system to design the RPSS to take care of the intra-area oscillations under perturbed conditions.

Also, the method developed in this paper can be used for power system stabilization & implementation in real time using dSPACE interfacing cards or DSP-TI Cards.

6. References

1. Chuanjiang Zhu, Member, Mustafa Khammash, Vijay Vittal, and Wenzheng Qiu: *"Robust Power System Stabilizer Design Using Loop Shaping Approach",* IEEE Trans. on Power Systems Analsyis, Vol. 18, No. 2, May 2003.
2. Yeonghain Chun, Takuhiko Ohashi, Yoichi Hori, Kook Hun Kim, Jong Bo Ahn, Seok Joo Kim: *"Robust Power System Stabilizer Design with H_∞ Optimization Method and Its Experiment on a Hardware Simulator",* IEEE Int. Conf. Paper, PCC-Nagaoka'97, pp. 741-746, 1997.
3. MacFarlane, D.C., and K. Glover, *"A loop shaping design procedure using H∞ synthesis",* IEEE Trans. on Automatic Control, Vol. AC-37, pp. 759–769, 1992.
4. Padiyar K.R.: *"Power System Dynamics - Stability and Control",* BS Publications, Second edition, Hyderabad, India, 2002.
5. Yao-nan Yu: *"Electric Power system Dynamics",* Academic Press 1983.
6. Kundur, P: *"Power System Stability and Control",* McGraw-Hill, New York, USA, 1993.
7. Padiyar K.R. and H.V. Saikumar: *"Modal Inertia - A New Concept for the Location of PSS in Multimachine Systems",* National Systems Conference, NSC-2003, India.
8. Mocwane,M, KA Folly*:" Robustness Evaluation Of H∞ Power System Stabilizer",* IEEE PES PowerAfrica 2007 - Conference and Exhibition Johannesburg, South Africa, 16-20 July 2007.
9. Ngamroo.I and S.Dechanupaprittha:*" Design of Robust H∞ Power System Stabilizer using Normalized Coprime Factorization",* The 2001 IEEE International Symposium on Circuits and Systems, 2001. ISCAS 2001.
10. Zhou, J.C., J.C. Doyle, and K. Glover: *"Robust and optimal control",* Prentice Hall Inc., New Jersey, USA, 1996.
11. Andrea Gombani and Michele Pavon: *"A general hankel-norm approximation scheme for linear recursive filtering",* Automatica, Vol. 26, Issue 1, pp. 103-112, Jan. 1990.
12. Doyle, J.C., B.A. Francis, and A.R. Tannenbaum, "Feedback control theory", Macmillan Press, New York, 1992.
13. Anderson P.M and Fouad A.A: *"Power system control and stability*", Iowa state university press, Ames, 1977.
14. Maciejowski, J.M : *"Multivariable feedback design",* Addison-Wesley publishing company.
15. Zhou, J.C., J.C. Doyle, and K. Glover: *"Robust and optimal control",* Prentice Hall Inc., New Jersey, USA, 1996.
16. Geir E. Dullerud and Fernando Paganini: *"A course in Robust Control Theory",* Springer-Verlag, 1999.
17. Tprkel Glad and Lennart Ljung:*"Control Theory: Multivariable and Nonlinear Methods",* Taylor and Francis publications.
18. Bouhamida, M., M.A. Denai, L.M. Ahed: *"Multivariable Robust Power System Stabilizer Design Based on H_∞"* Proceedings of International Power Electronics and Motion Control Conference, 2000.

Appendix

A. Equations of Multi-Machine Power System of the Model 1.1

In multi-machine power system, each machine is expressed in its own d-q ref. frame which rotates with its rotor. For solving interconnecting network equations, all voltages and currents are expressed in a common reference frame rotating at synchronous speed (*D-Q* or Kron's reference frame). Axes transformation equations are used to transform between individual machine (*d-q*) reference frames and the common (*D-Q*) reference frame.

The equations of multi-machine power system corresponding to the Model 1.1 including saliency are given as follows [4]. Each parameter in these

equations is a vector or matrix.

$$[T'_{d0}]\frac{d[E'_q]}{dt}=\{-[E'_q]+([x_d]-[x'_d])[i_d]+[E_{fd}]\}$$

$$[T'_{q0}]\frac{d[E'_d]}{dt}=\{-[E'_d]-([x_q]-[x'_q])[i_q]\}$$

$$\frac{d[\delta]}{dt}=\omega_B([S_m]-[S_{mo}])$$

$$\frac{d[S_m]}{dt}=\frac{1}{2[H]}([T_m]-[D][S_m]-[T_e])$$

$$[T_e]=[E'_d][i_d]+[E'_q][i_q]+([x'_d]-[x'_q])[i_d][i_q]$$

$$\begin{bmatrix}[i_d]\\ [i_q]\end{bmatrix}=\begin{bmatrix}[R_a] & [x'_q]\\ -[x'_d] & [R_a]\end{bmatrix}^{-1}\begin{bmatrix}[E'_d]-[v_d]\\ [E'_q]-[v_q]\end{bmatrix}$$

$$[T_a]\frac{d[E_{fd}]}{dt}=[[K_a]([V_{ref}]+[V_S]-[V_t])-[E_{fd}]]$$

The rotor angle and speed with COI reference are given by

$$\delta_{COI}=\frac{1}{M_T}\sum_{i=1}^{n}M_i\delta_i\ ;\ \omega_{COI}=\frac{1}{M_T}\sum_{i=1}^{n}M_i\omega_i$$

$$M_T=\sum_{i=1}^{n}M_i$$

If transient saliency is considered, then the current equation can be expressed after transforming into *D-Q* reference frame, we get

$$\begin{bmatrix}i_Q\\ i_D\end{bmatrix}=[Y_g^{DQ}(t)]\begin{bmatrix}E'_Q-v_Q\\ E'_D-v_D\end{bmatrix}\text{ Where}$$

$$[Y_g^{DQ}(t)]=\frac{1}{(R_a+jx'_dx'_q)}\times\begin{bmatrix}\cos\delta & -\sin\delta\\ \sin\delta & \cos\delta\end{bmatrix}\times\begin{bmatrix}R_a & x'_d\\ -x'_q & R_a\end{bmatrix}\begin{bmatrix}\cos\delta & \sin\delta\\ -\sin\delta & \cos\delta\end{bmatrix}$$

$[Y_g^{DQ}]$ is a function of δ and as δ varies with time *t*, it becomes a time varying matrix. Hence, special technique is required to handle transient saliency using two ways.

1. Using a dependent source E'_{dc} such that

$$E'_{dc}=-(x'_q-x')_d\,i_q$$

It can be shown that

$$\hat{I}_g=Y_g\left[E'_q+j\,(E'_d+E'_{dc})\right]e^{j\delta}$$

where $Y_g=\dfrac{1}{R_a+j\,x_d^1}$

2. Using a dummy rotor coil such that E'_{dc} is a state variable proportional to flux linkage of a dummy coil in the *q*-axis. The differential equation for E'_{dc} can be expressed as

$$[T'_c]\frac{d[E'_{dc}]}{dt}=\{([x'_d]-[x'_q])[i_q]-[E'_{dc}]\}$$

The load at a bus can be represented by the equivalent circuit shown in Figure 13 where the load admittance Y_l is given by $Y_l=\dfrac{P_{L_0}-jQ_{L_0}}{V_{L_0}^2}$

The network equations can be expressed using bus admittance matrix Y_N as

$$[Y_N]\hat{V}=\hat{I}_N$$

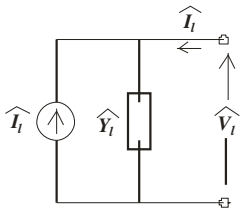

Fig.17 Equivalent circuit representation of load

Where $\hat{V}$ is a vector of complex bus voltages. The generator and load equivalent circuits at all the buses can be integrated into the AC network and the overall system algebraic equations can be expressed as $[Y]\hat{V}=\hat{I}$

In *D-Q* reference frame this equation can be expressed as

$$[Y^{DQ}]\ V^{DQ}=I^{DQ}\quad\text{Where}$$

$$V^{DQ}=\begin{bmatrix}V_D\\ V_Q\end{bmatrix}=\begin{bmatrix}Z_R & Z_I\\ -Z_I & Z_R\end{bmatrix}\begin{bmatrix}I_D\\ I_Q\end{bmatrix}$$

where $[Z_R+jZ_I]=[Z]=[Y]^{-1}$ and $[Y]$ is the complex admittance matrix which is obtained by augmenting the bus admittance matrix Y_N by shunt admittance Y_g of generator and load admittances at the generator and load buses Y_l. The elements of Y_{ij}^{DQ}, V_j^{DQ} and I_i^{DQ} can be expressed as

$$[Y_{ij}^{DQ}]=\begin{bmatrix}B_{ij} & G_{ij}\\ G_{ij} & -B_{ij}\end{bmatrix},\ V_j^{DQ}=\begin{bmatrix}V_{Qj}\\ V_{Dj}\end{bmatrix}\text{ and }\ I_i^{DQ}=\begin{bmatrix}I_{Di}\\ I_{Qi}\end{bmatrix}.$$

B. The Simulink Model

The developed Simulink model of the IEEE 10 machine, 39 bus multi-machine power system considered for designing RPSS using Glover McFarlane H_∞ loop shaping technique and to study the control of power system oscillations, is shown in the Fig.18. The developed RPSS connected to generators 1, 5, 7, 8 and 9, through mux and demux is shown in Fig.19.

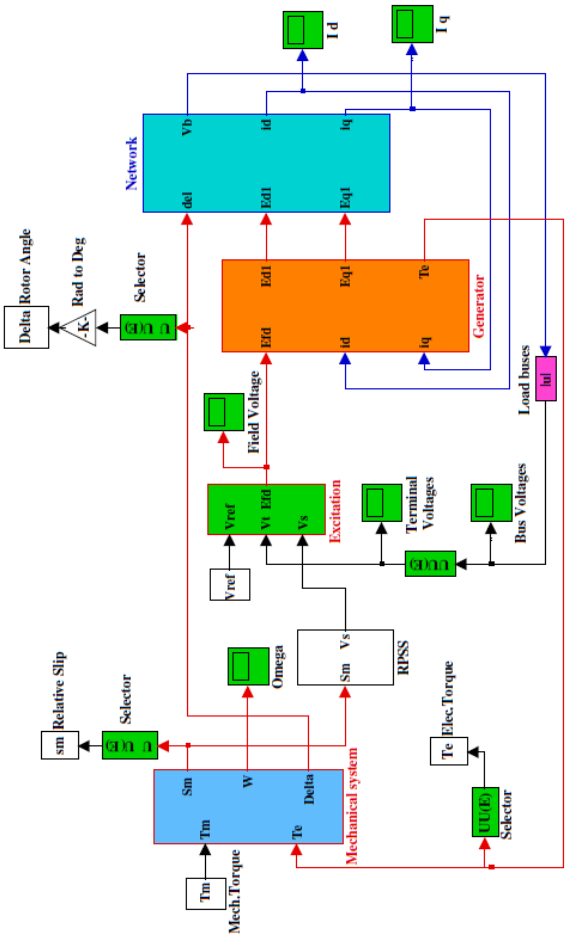

Fig.18 The developed Simulink model of the multi-machine power system represented by the Model 1.1 including saliency with RPSS

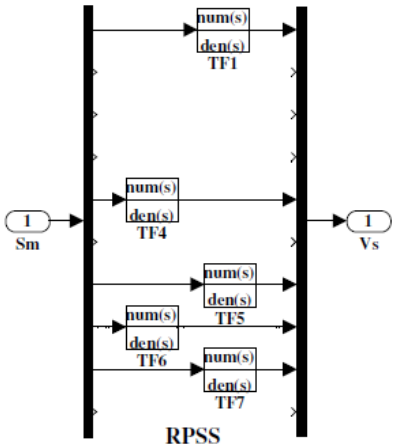

Fig.19 The developed RPSS connected to generators 1, 5, 7, 8 and 9, through mux and demux.

In Fig.18, multiple data corresponding to the number of generators or buses flow in each line. Selectors are used to tap the data corresponding to any generator or bus. The data related to rotor angle, relative slip and electric torque are connected to workspace and results are plotted using plot() function. The other parameters, if necessary, can be observed using scopes.

C. The Data

The single line diagram of 10-M/c, 39 bus multi-machine power system [4] is shown in Fig.20. The machine data, excitation data, line data, load flow data and transformer data can be referred from [4].

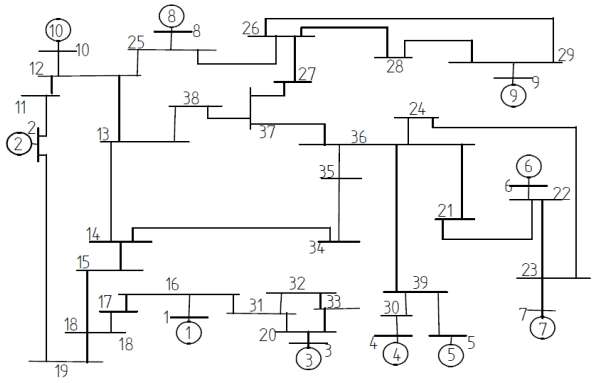

Fig.20 Single line diagram of the 10-Machine, 39-bus Multimachine Power System

D. The CPSS

The schematic representation of Conventional Power System Stabilizer (CPSS) is as shown in the Fig.21.

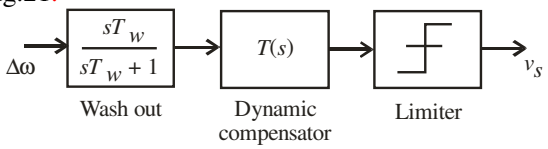

Fig.21 Conventional Power System Stabilizer

In the block diagram of the CPSS shown, the transfer function $T(s)$ is finally obtained as $T(s) = \dfrac{Ks(1+sT_1)(1+sT_3)}{(1+sT_2)(1+sT_4)}$. The designed parameters of CPSS for the system considered are $K_s = 15$, $T_1 = 0.75\,s$, $T_2 = 0.3\,s$, $T_w = 10$ Limits on V_s as $+0.05$ & -0.05.